THE EFFECT OF SLAT AND FLAP TO THE AERODYNAMICS PERFORMANCE OF AN AIRFOIL

MOHD SOFIAN BIN ABD HAMID

Report

Projek Sarjana Muda 2

Supervisor : DR NAZRI BIN MD DAUD

Second Examiner : DR FADHLI BIN SYAHRIAL

Faculty Of Mechanical Engineering

Universiti Teknikal Malaysia Melaka

2017

DECLARATION

I declare that this project entitled "The effect of slat and flap to the aerodynamic performance of an airfoil" is the result of my own work except as cited in the references.

Signature : .....

Name : MOHD SOFIAN BIN ABD HAMID

Date : 24 MAY 2017

APPROVAL

I have checked this report and the report can now be submitted to JK-PSM to be delivered back to supervisor and to the second examiner. DR NAZRI BIN MD DAUD

Signature	:	.....
Name of Supervisor	:	DR NAZRI BIN MD DAUD
Date	:	24 MAY 2017

DEDICATION

I dedicate this project to my beloved parents.

ABSTRACT

This study was dealing with the effect of the application of the leading edge slat and trailing edge flap on the NACA 0015 airfoil. The lift and drag coefficient were determined after some experiments and further calculation based on the theoretical formula. Generally it is about to see the difference of the airfoil characteristic when it is not equipped with the slat and flap and when the airfoil is being equipped with the slat and flap. The experiment took place in a subsonic high velocity wind tunnel. The airfoil was set up at the angle of attack from 0 to 20 with the 5 of interval. The wind tunnel was set with a constant air velocity of 9.5m/s. The indicator panel on the wind tunnel will show the value of lift force and drag force. The data was recorded and the n the experiment is proceed with the replacement of the airfoil with the modified airfoil with the slat and flap. Several configuration of the slat and flap with variety combination of angle of attack was set and tested. The data was recorded. From the test it was found the best angle of attack combination of the slat and flap that is the best for the airfoil. Slat with the angle of 30 with the flap with the angle of 0 gives the best lift force on the airfoil with the value of the lift coefficient of 1.006. hence it can be conclude that the leading edge slat and trailing edge flap can affect the aerodynamic performance of an airfoil.

ABSTRAK

Kajian ini berkaitan dengan kesan penggunaan flap pinggir hadapan dan belakang pada aerofoil NACA 0015. Daya ngkat dan seret ditentukan selepas beberapa eksperimen dan berdasarkan formula teori. Secara umumnya ia adalah kira-kira untuk melihat perbezaan ciri aerofoil apabila ia tidak dilengkapi dengan bertampar dan flap dan apabila aerofoil sedang dilengkapi dengan bertampar dan flap. percubaan itu berlaku di dalam terowong angin halaju tinggi subsonik. aerofoil ditubuhkan pada sudut serang 0-20 dengan 5 selang. Terowong angin telah ditubuhkan dengan halaju udara yang berterusan daripada 9.5m / s. Panel penunjuk pada terowong angin akan menunjukkan nilai daya angkat dan daya seret. data telah dicatat dan n eksperimen adalah meneruskan penggantian aerofoil dengan aerofoil yang diubah suai dengan bertampar dan flap. Beberapa konfigurasi slat dan flap dengan kombinasi pelbagai sudut serang ditubuhkan dan diuji. data telah dicatat. Daripada ujian didapati sudut terbaik kombinasi serangan slat dan flap yang terbaik aerofoil. Bertampar dengan sudut 30 dengan kepak dengan sudut 0 memberikan daya angkat terbaik di atas aerofoil dengan nilai pekali daya angkat daripada 1,006. oleh itu ia boleh membuat kesimpulan bahawa flap pinggir hadapan tepi bertampar dan belakang boleh menjejaskan prestasi aerodinamik aerofoil.

ACKNOWLEDGEMENT

First thing first, I would like to give my whole heartedly thank you to my supervisor for this study, Dr Nazri bin Md Daud. As my research supervisor, he was such a good mentor and without his helps I will not able to finish my research right on time. He guided me from the beginning until the last minutes of this research. He has helped and supported me to complete my research.

Besides that, not being forgotten my parents in Johor. My father Abd Hamid bin Aini. My mother Saropah binti Warjan. These two people is the one who have helped me a lot not only for this research but from the beginning of everything. They always encourage me to always give my best in everything. They are also believe in me and always motivate me to be a better person.

Next, I would like to give thousands of thank to someone special. To my fiancé Noor Syazwani binti Soelastro who were always be here with me supporting me and keep motivate me to finish my research and give my best on this research. She was always be on my side especially when I was having my difficult time and keep encourage me to not give up. Thank you.

And lastly, I would like to acknowledge with much appreciations to friends for their continuous support and encouragement throughout the project period. To all my BMCT friend, my FKM friend and all my UTeM friend.

TABLE OF CONTENTS

LIST OF FIGURES

LIST OF TABLES

LIST OF ABBEREVATIONS

DBD	Dielectric barrier discharge
PVC	Polyvinyl chloride
PMMA	Polymethyl methacrylate
PIV	Particle Image Velocimetry

CHAPTER 1

INTRODUCTION

1.1 Background

Flap was originally being invented and applied to the airfoil purposed to improve the take off and landing aerodynamics process of an airplane. The optimization results show that under takeoff configuration, the variable camber trailing-edge flap can increase lift coefficient by about 8% and lift-to-drag ratio by about 7% compared with the traditional flap at a takeoff angle of 8°. (Weishuang, Yun, & Peiqing, 2017). In these few years back, the more attentions are given to the aerodynamics of deformable wings. The term deformable means that the wings have flap that can be retracted back (Li, Dong, & Liu, 2015).

Leading edge slat and the trailing edge flap are commonly being applied on the airfoil wings in order to obtain high lift force towards the wings. The design of this type of wings are aided by modern numerical modelling that able people to evaluate many value of performance on different geometries (Savory, Toy, Tahouri, & Dalley, 1992).

1.2 Problem statement

The fuel usage efficiency of an aeroplane is normally being affected by many factors such as the distance, the velocity and the drag force. Basically, the drag force acting on the body of the aeroplane especially the wings give the greatest impact to the fuel consumption. The drag force will slow the velocity of the plane down, more power will be used to overcome the drag

because they have and estimated time to arrive to be followed. Using extra power on the engine will directly increase the fuel consumption of the plane.

There were many researches done before working on how to solve this problem. For example, in 1990, Mohamed Gad-El-Hak has done a research on control of a low-speed airfoils aerodynamics in order to find solutions for the problem encountered. Some famous research regarding to the problem of the drag force of an aeroplane's wings is about designing an aerodynamic shape of the wings. A different shape will give different measure related to the flow around it. For example, a bluff area will cause greater air resistance compared to the one with aerodynamic shape.

The application of slatted leading edge of an airfoil and the flapped trailing edge of an airfoil is one of the thing that is being study in order to have a better performance of an airplane. With the theory that the application of flap and slat that is able to increase the lift of an airplane, it means that lower velocity is needed for the airplane to take off which also means that less fuel consumption during the take off. The flap is affecting for the take off while the slat is for the cruising ship at constant velocity.

1.3 Objective

The objectives of this project are as follows :

1. To study the effect that can be caused by the application of leading edge slat and trailing edge flap on NACA 00115 airfoil,
2. To evaluate the drag and the lift of the NACA 0015 airfoil.
3. To compare the result of the application of slat and flap to the one with no flap and slat.

1.4 Scope of project

The scopes of this project are as follows:

1. Design and fabricate a NACA 0015 airfoil
2. Testing the normal NACA 0015 airfoil with no slat and flap in a high velocity wind tunnel.
3. Testing the modified NACA 0015 airfoil with slat on the leading edge and flap on the trailing edge in a high velocity wind tunnel.

1.5 General methodology

The actions that is needed to be carried out in order to achieve the objectives of this project are listed below:

1. Literature review

   Journals, articles, or any materials regarding to this project will be reviewed to find extra information related to the effect of the plasma actuator to the airfoil.

2. Experimentation

   Experiments will be conducted to test the effect of the application of slat on the leading edge of the airfoil and flap on the trailing edge of the airfoil. The cross sectional drawing of this airfoil with slat and flap can be seen as in Figure 1.5.1. The general overview of this project can be seen through the flowchart of this study (Figure 1.5.2)

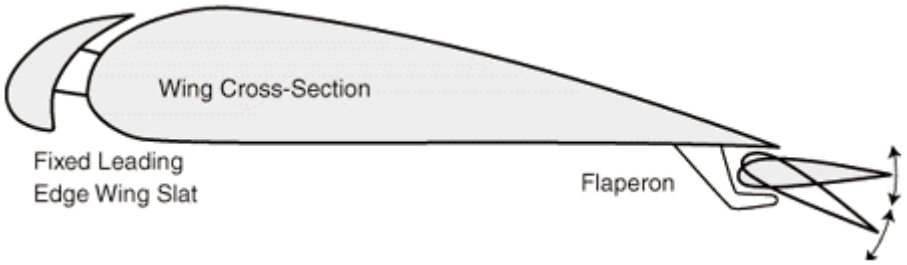

Figure 1.5.1 The cross sectional diagram of the setup of the NACA 0015 airfoil with the lading edge slat and trailing edge flap (Weishuang et al., 2017)

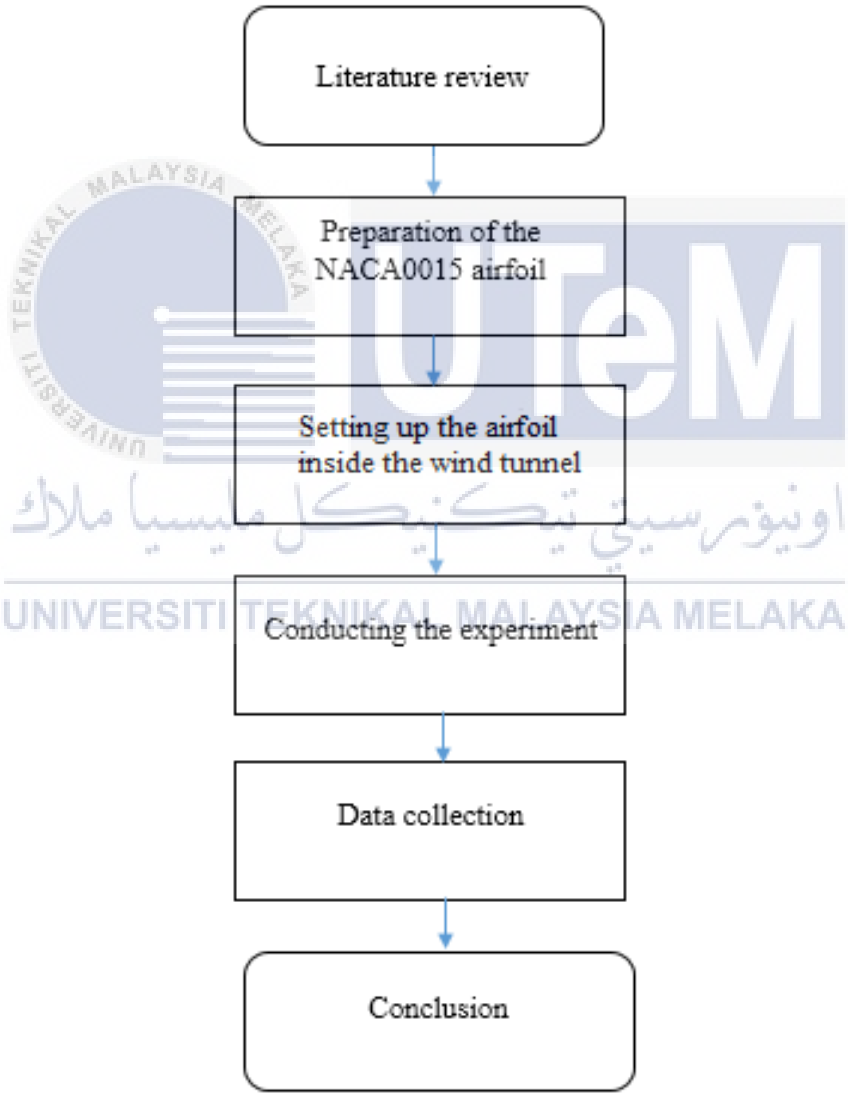

Figure 1.5.2 The overall flowchart of this research

CHAPTER 2

LITERATURE REVIEW

2.1 Introduction

In this chapter, a few previous studies done related to the effect of application of the leading edge slat and the trailing edge flap will be reviewed here to gather as much as information that can be very helpful in the future.

2.2 Leading edge slat and trailing edge flap

Trailing-edge flap is traditionally used to improve the takeoff and landing aerodynamic performance of aircraft. In order to improve flight efficiency during takeoff, cruise and landing states, the flexible variable camber trailing-edge flap is introduced, capable of changing its shape smoothly from 50% flap chord to the rear of the flap (Weishuang et al., 2017) Flapping-wing offers unique force-producing mechanisms over conventional flight methods for designing micro air vehicles, especially in the low Reynolds number (Re) regime. (Dickinson et al., 1999)

Figure 2.2.1 An A-300 series airfoil profile with leading edge slat and trailing edge flap (Savory et al., 1992)

Aircraft wing design generally takes the efficiency of the cruise flight and the high-lift performance at takeoff and landing into consideration and the trailing-edge high-lift devices have been widely used on many kinds of aircraft previously (Li et al., 2015)

2.3 Experimental design and set up

In his current study, Lu Weishiang used the GA (W)-2 airfoil is as an analytical model; this is an advanced airfoil for general aviation with a maximum thickness of about 13% of its chord, c. The configuration for the take off and landing mechanism for this airfoil are as in Figure 2.3.1 below where d df is the deflection angle of the flap, xp is the translation amount in the horizontal direction and zp is the translation amount in the vertical direction

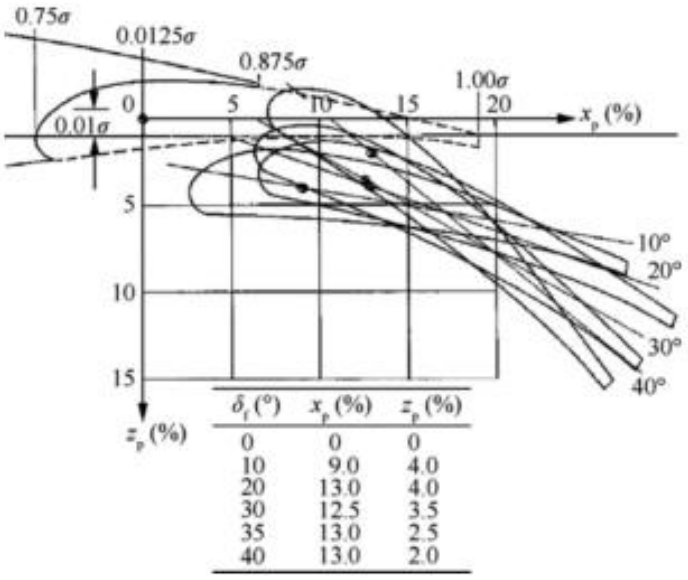

δ_f (°)	x_p (%)	z_p (%)
0	0	0
10	9.0	4.0
20	13.0	4.0
30	12.5	3.5
35	13.0	2.5
40	13.0	2.0

Figure 2.3.1 Configuration for takeoff and landing of a GA (W)-2 airfoil. (Weishuang et al., 2017)

In a different but related paper, the writer W.L Siauw in his paper entitled Transient phenomena in separation control over a NACA 0015 airfoil, NACA 4412 was used as a model in his experiment. The test section was 1.3m high, 1.7mwide and 3.0m long. The contraction ratio was 1:8 and the flow was driven by an eight- blade axial fan. The vertically mounted model spanned the entire working section. The model ends were attached to horizontal turntables placed in the central part of the working section. The lower turntable enabled the manual adjustment of the airfoil angle of attack. Porous plates were installed on both lower and upper turntables, through which suction was applied along the model suction-side and in front of the slat to reduce the effect of the tunnel wall boundary layer.

The main wing, slat, and flap were provided with a total of 270 tappings along the centerline to permit the measurement of comprehensive pressure distributions and the computation of overall drag and lift forces(Savory et al., 1992) The experiments were conducted in a blowdown wind tunnel, with working section dimensions of 1.68 m height × 1.37 m width × 9.0 m length and a free-stream turbulence level of 0.20%. A free-stream velocity of 20 m/s was used, giving a chord Reynolds number of 1.26 × 10 6. Only two configurations have been studied to date: with the high-lift devices with- drawn and with the slat and flap set at their optimum posi- tions (slat angle of 25° and flap angle of 20° to the main wing)

Figure 2.3.2 Schematic view of the 270 pressure tappings distributed along the airfoil chord (Pagani, Souza, & Medeiros, 2017)

The top view of the airfoil arrangement and the angle of attack inside the wind tunnel are as in the Figure 2.3.3

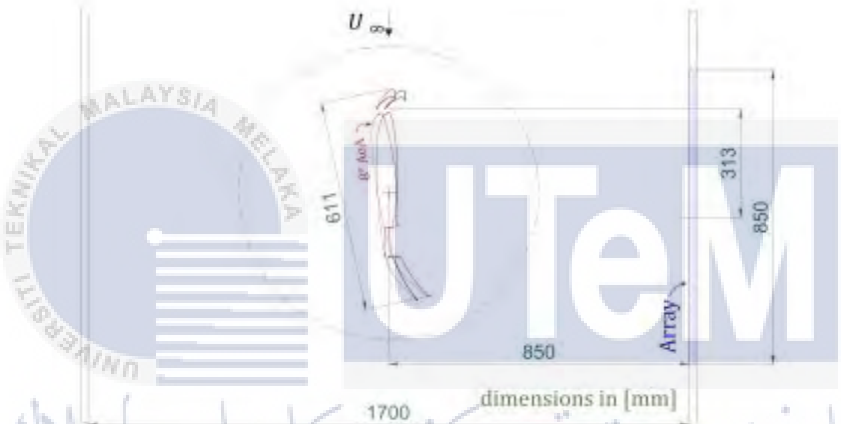

Figure 2.3.3 Top view of the airfoil inside wind tunnel with its angle of attack (Pagani et al., 2017)

Sahin in his paper Numerical and Experimental Investigations of Lift and Drag Performances of NACA 0015 Wind Turbine Airfoil, has conducted an experiment in an open wind tunnel at the University of Gazi, Faculty of Technology. This tunnel test section long is about 0.4m long and flow cross- section is approximately 0.3m×0.3m, interval of wind velocity is from 3.1 to 28 m/s. The airfoil profile used in his experiment was the NACA 0015 airfoil.

Figure 2.3.4 The wind tunnel (Şahin & Acir, 2015)

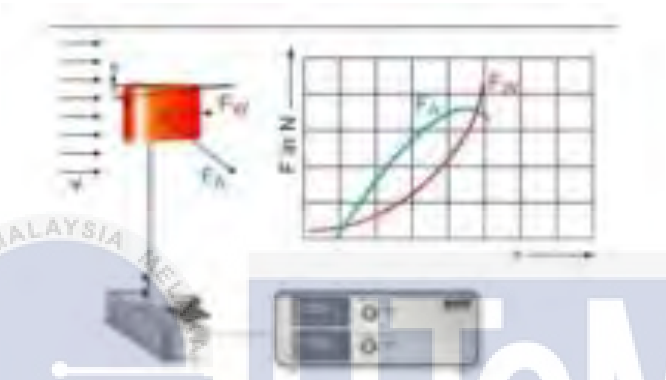

Figure 2.3.5 Wind tunnel test mechanisms (Şahin & Acir, 2015)

The experiments has been conducted at 10 m/s wind velocity (V) in tunnel which is corresponding to 68490 Reynolds number (Re) and the airfoil is forced stationary wind velocity to learn lift and drag coefficient, the airfoil profile is attached to electronic two- component coefficient transducer. The values for drag and lift are displayed digitally on the measurement amplifier (Şahin & Acir, 2015)

2.4 Result and discussion

From the ANSYS FLUENT analysis, Lu Weishuang said that at an attack angle below 19, the total lift coefficient of the airfoil increases with the angle of attack, agreeing well with experimental results. The aerodynamic forces of the leading-edge slat wing and main body and trailing-edge flap are also in good agreement with experiment and then the angle of attack is

greater than 19°, the calculated lift coefficient of the leading-edge slat wing is larger, making the calculated lift coefficient of the multi-airfoil become relatively larger, and the stall angle of attack is around 23°, which represents an increase of about 2° compared with the experimental data. Figure 2.4.1 shows a comparison of the pressure coefficient distribution, Cp, obtained by numerical simulation and by wind tunnel test results when the angle of attack is 8°. And The wakes of the main body obtained by both experiment and numerical simulation can be seen from Figure 2.4.2.

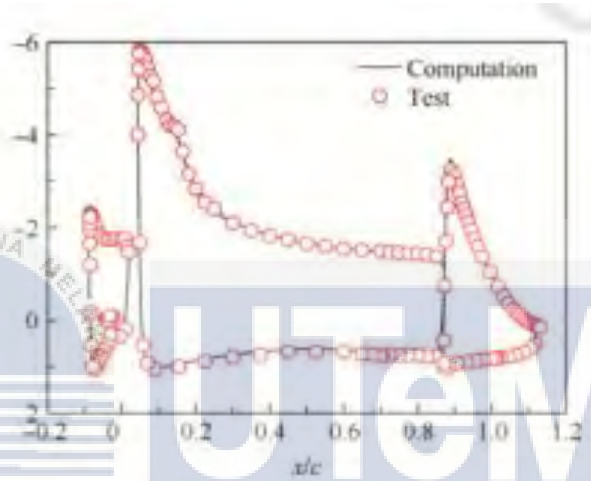

Figure 2.4.1 The comparison of Cp for simulation and numerical.(Weishuang et al., 2017)

Numerical simulation of the speed loss of the wake of the slat clearly exceeds its experimental value. When the angle of attack is 8°, the boundary layer of the main section (x=0.45c) is plump and uniform, whereas that of the flap section is not, which is consistent with the pressure-coefficient curves.

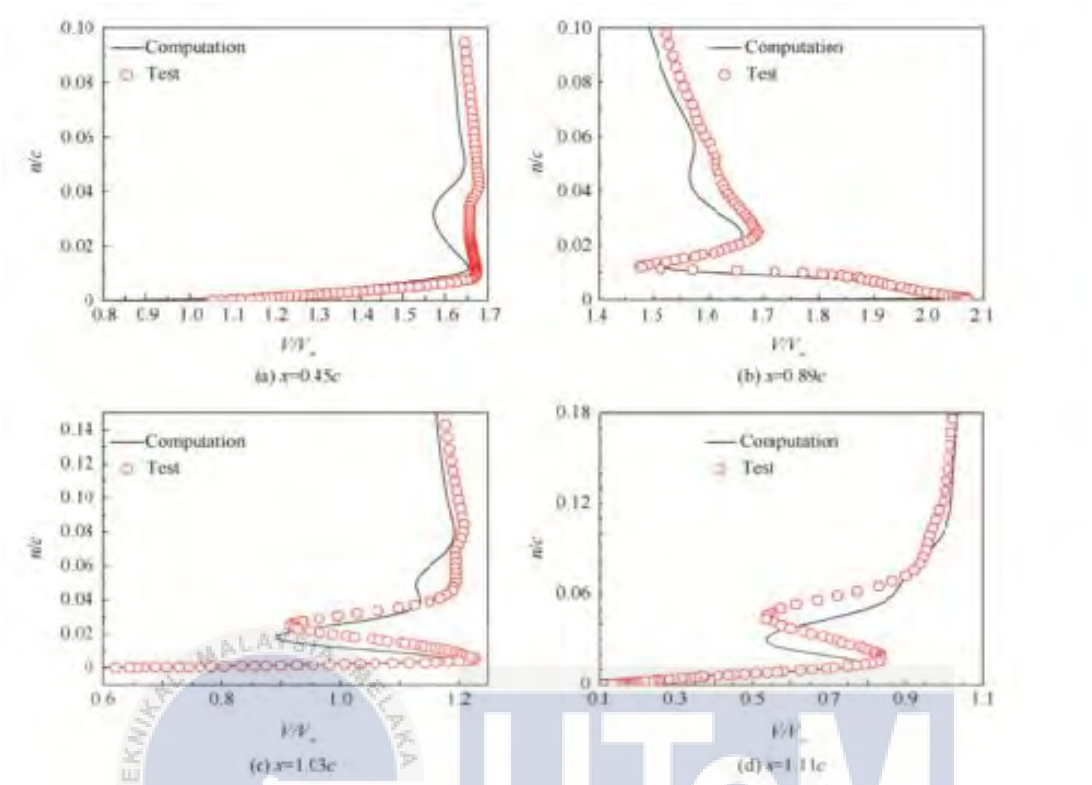

Figure 2.4.2 Velocity profile for the cross sectional airfoil .(Weishuang et al., 2017)

From the paper pf Flow Regimes in the Cove Regions Between a Slat and Wing and Between a Wing and Flap of a Multielement Airfoil by E. Savory, a lift coefficient of approximately 4 at an incidence of 20° is consistent with that expected from previous work on A-300 series geometries with similar slat and flap arrangements. The streamlines approaching the slat and the acceleration of the flow through the cove region is shown as in figure 2.4.3 and the extent of the recirculation region behind the slat when it is deployed at 25° to the chord line is illustrated in Figure 2.4.4.

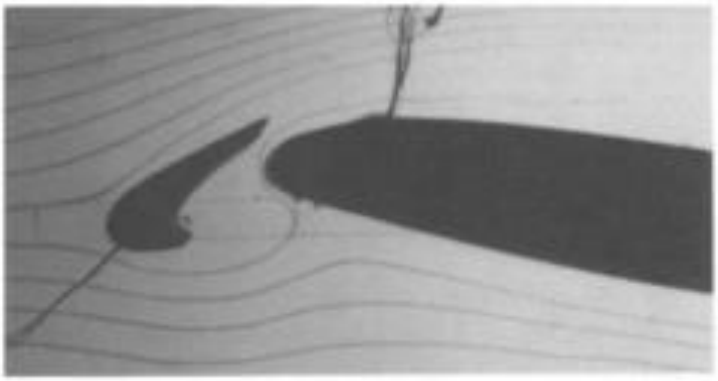

Figure 2.4.3 The streamlines around the extended slat (Savory et al., 1992)

Figure 2.4.4 Recirculation region behind the extended slat. (Savory et al., 1992)

The overall lift and drag coefficient curves for the two configurations are illustrated in Figure 2.4.5.

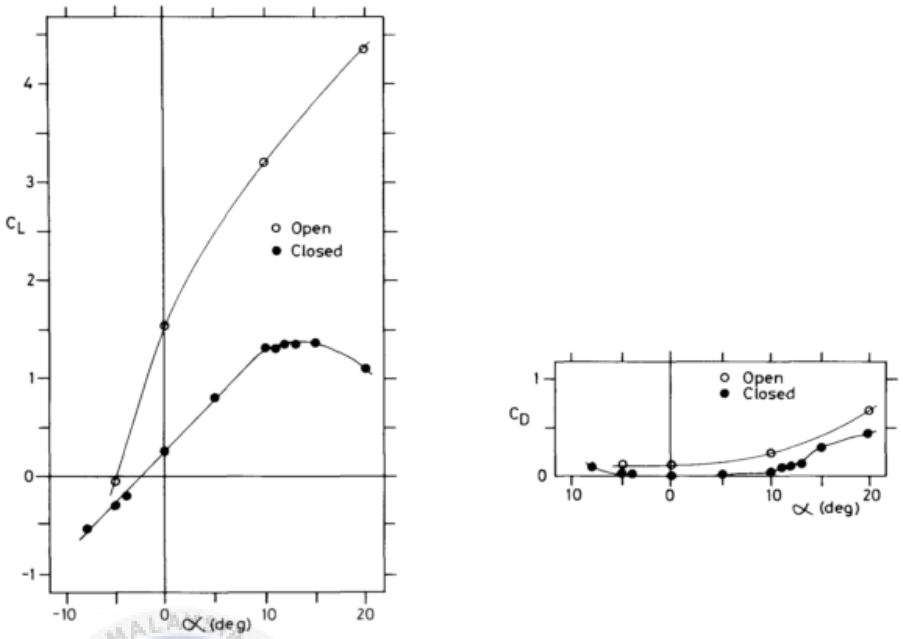

Figure 2.4.5 Lift and drag curves for the airfoil with the devices open and close (Savory et al., 1992)

Sahin and Adem in his paper stated that they performed the experiment and analysis method and the experiments were conducted at 10 m/s wind velocity. Lift and drag coefficient of NACA 0015 airfoil at different attack angle between 0° and 20° were measurement. Also, the lift and drag coefficient were obtained as numerical with FLUENT programs for the same conditions. Airfoils have various shape and sizes. Therefore, non–dimensional coefficients (lift and drag coefficients) were taken into consideration to evaluate the advantages and disadvantages of airfoils.

The lift and drag coefficient at wind tunnel test for NACA0015 airfoil were measured as experimentally and he maximum lift and drag coefficient were found as 0.75 and 0.15 for 16° attack angle(Şahin & Acir, 2015) Spalart Allmaras method showed similarity experimental results as illustrated in Figure 2.4.6.

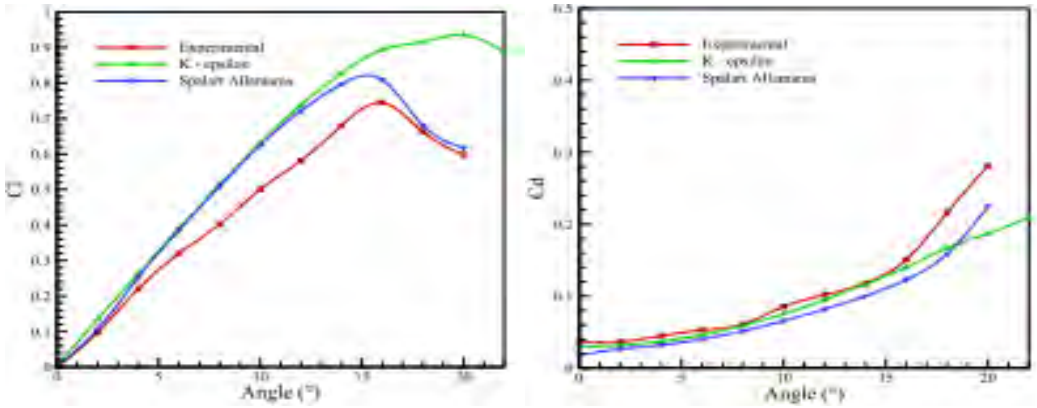

Figure 2.4.6 Experimental and numerical analysis

The flow was laminar around the NACA 0015 airfoil between 0° to 14° angle of attack. Laminar flow was transition turbulence flow and pressure distribution changed around 16° angle of attack so lift coefficient began decrease.

And lastly to conclude their study, writers stated that the optimum lift coefficient value was measured and computed at 16°. The optimum airfoil performance was measured and calculated at about 8°. Experimental and numerical analysis were shown a good results and similarity.

CHAPTER 3

METHODOLOGY

3.1 Overview

This chapter discusses the whole methodology throughout this research on study the effect of the application of leading edge slat and trailing edge flap on the NACA0015 airfoil. The methodologies cover from the beginning of the research which is studies on previous research until the end of data collection from the experiments.

3.2 Introduction

From the studies of the previous research, we can roughly conclude that the application of the slat and flap can alter few parameters of the flow around the airfoil such as the pressure distribution and the velocity profile. To prove the early conclusion, a further research should be conducted. There will be few main stages in this research which are the preparation of the airfoil NACA0015, setting up the apparatus in the wind tunnel, conducting the experiment and collecting the data.

3.3 Flow chart

Flowchart is purposed to give an overview of the steps involved during research. It is important to show the correct sequences and the pathway during the research if there is a conditions that can give two or more results. The flowchart for this study can be seen as in figure 3.3.1

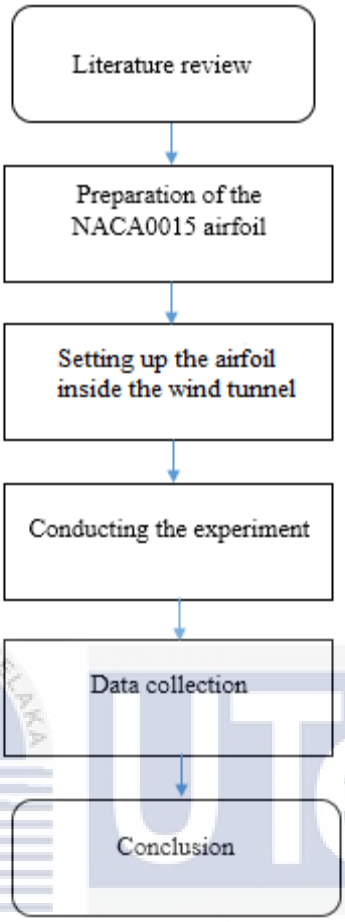

Figure 3.3.1 The flowchart of this research

3.4 Literature review

A research has been done earlier regarding to the effect of the slat and flap ont the airflow of NACA 0015. Many previous research papers had been studied properly. The aspects that were given more attention on the previous research paper were the experimental set up, the methods on collecting data and the results. A more detailed about the gain from the studies was discussed in the previous chapter.

3.5 Preparation of NACA 0015 airfoil

The NACA airfoils are airfoil shapes for aircraft wings developed by the National Advisory Committee for Aeronautics (NACA). The shape of the NACA airfoils is described using a series of digits following the word "NACA". The NACA airfoil that will be used in this research is NACA 0015 airfoils. The preparation of this airfoil is started with the coordinate of the airfoil. This airfoil can not be sketched randomly because the aspect ratio of the length of chord, the thickness of the airfoil and the curve of the surface is fixed. Slightly change in measurement will change the airfoil shape. The coordinates for the plotting of the airfoil sketch can be obtained from the website airfoiltools.com. (Fig. 3.5.1). After that, we can select from the various type of NACA airfoils in the database. After selecting the type of airfoil, we can enter our custom properties of the airfoil such as the length of the chord and the colour (Fig. 3.5.2). For this research NACA 0015 is being used and we set the length of chord to 100mm. after entered the desired details, the website will generate the coordinates for plotting the airfoil (Fig. 3.5.3). The coordinates will be used later in SolidWorks software to draw the airfoil (Fig. 3.5.4). After open the software, we start with open new file for drawing single component (Fig 3.5.5) and then select the curves tab and click on the curves through XYZ point (Fig.3.5.6). After clicked that, a new window will be opened (Fig 3.5.7) and then we just insert the coordinates obtained from the website. Done inserting the coordinates, the drawing of the airfoil will come out and so that we can proceed to extrude the two dimensions drawing into solid three dimensions model (Fig 3.5.8) During the extrude option, we can select the length of the span of the airfoil by entering the desired length at extrude length tab and press OK and a solid model of a NACA 0015 airfoil is created. The solid model produced on the computer will later on being brought to the 3D printing machine to produce a real solid model of an airfoil that will be used for this experiment. The dimensions of this airfoil are 100mm chord length with a 150mm span length.

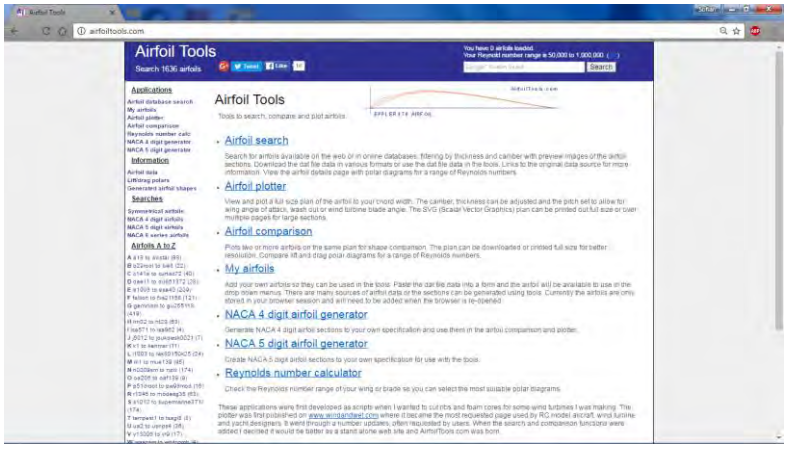

Figure 3.5.1 The interface of the home of the airfoiltools website

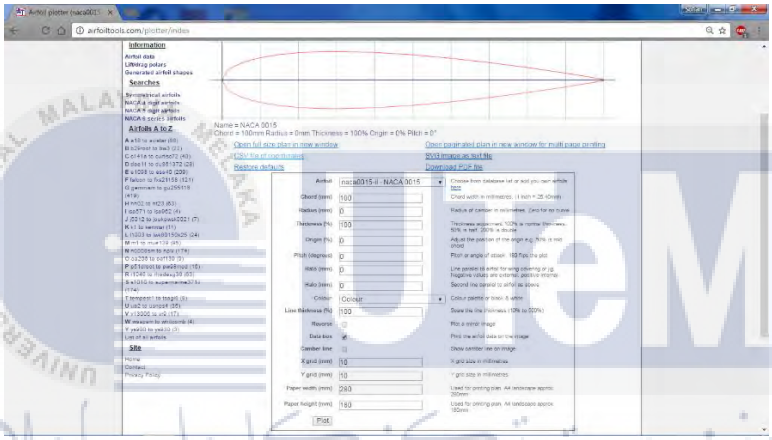

Figure 3.5.2 Insert the properties of the desired airfoil

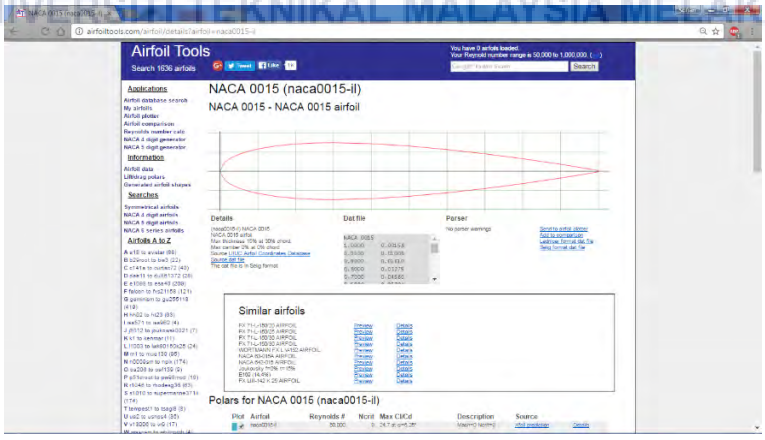

Figure 3.5.3 The coordinates generate for plotting the airfoil shape

Figure 3.5.4 Interface of the start up the SolidWorks software

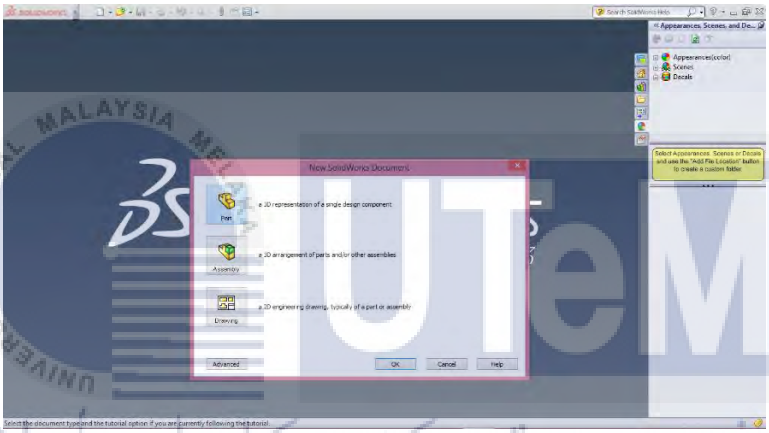

Figure 3.5.5 Selecting the drawing of a single component

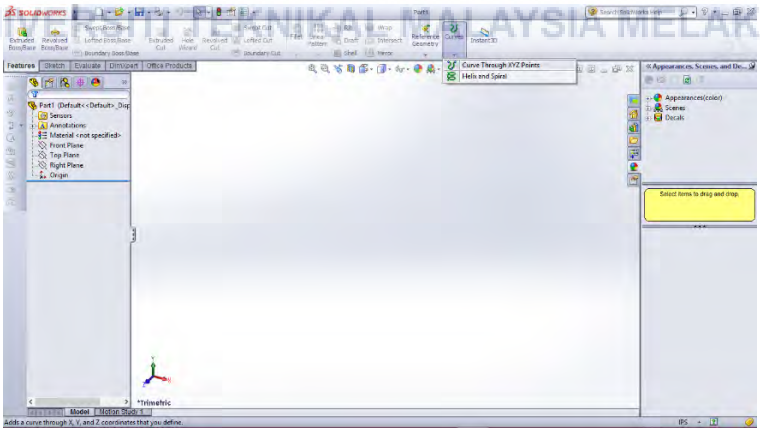

Figure 3.5.6 Selecting the curves from XYZ points from the Curves tab

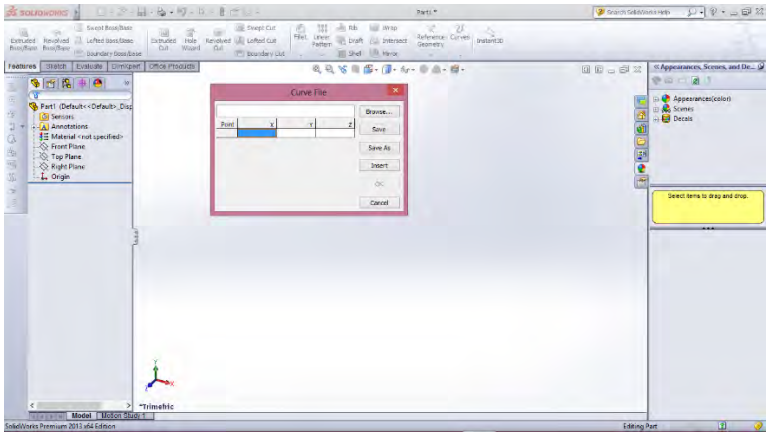

Figure 3.5.7 Inserting the coordinates of X, Y and Z axis of the airfoils

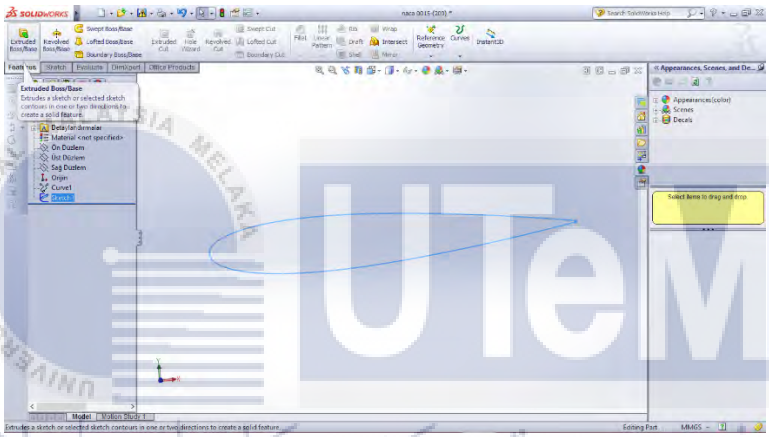

Figure 3.5.8 Shape of the airfoil generated from the coordinates and selecting the extrude feature

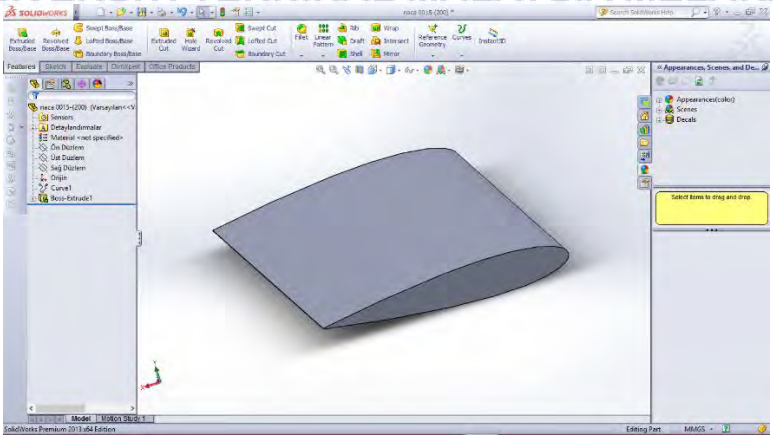

Figure 3.5.9 Solid model of NACA 0015 airfoil generated

After done with the computer modelling, we will proceed next with the printing session. The model was printed at the innovation and prototype laboratory at the Kompleks Makmal Kejuruteraan Mekanikal Fasa B UTeM. The printing system here is using the CubePro Duo. The model file which is the SolidWorks file is first being access using the computer that is connected to the printer. Using the CubePro Duo software in the computer, we can setting the sizing of the model to be printed. We can print smaller prototype or even larger size prototype rather than the size in the programming. The printing machine (Figure 3.5.10) is able to print a model up to 30cm x 30cm x 30cm in size.

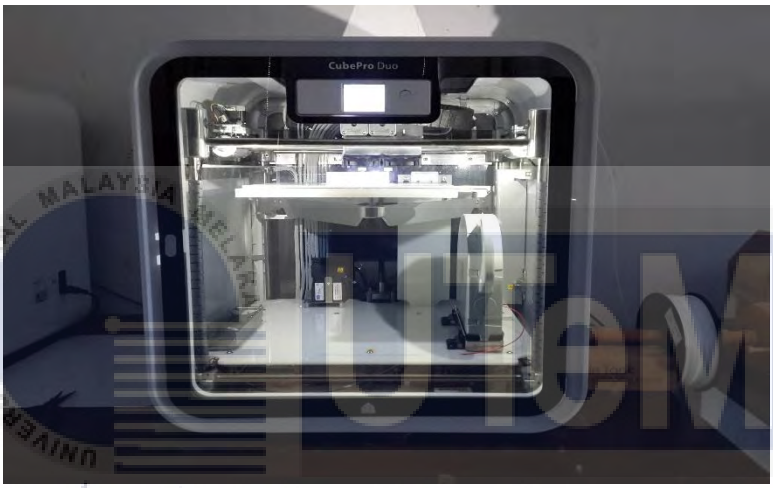

Figure 3.5.10 The CubePro Duo 3D Printing machine

The material used for this printing is the acrylonitrile butadiene styrene (ABS) as in Figure 3.5.11. We bought 1kg of the ABS material for the printing. The ABS come in a roll of 1kg as it is in a wire like shape (Figure 3.5.11). The roll of ABS is then being inserted inside the printer connected to the nozzle that will move and shape the model. This model required 6 hours of printing. After done with the printing of the airfoil, the printing stage for the slat and flap of the airfoil. The same step was done as in printing the airfoil model. After finish with the printing of the model parts, we attached the slat and flap to the airfoil to produce our main thing in this study which is an airfoil with flap and slat (Figure 3.5.12)

Figure 3.5.11 The ABS for the printing material

Figure 3.5.12 Printed model of NACA 0015 with flap and slat

The printed model of the airfoil is then will be used throughout the studies. Series of configuration of the airfoil with its slat and flap will be tested in the wind tunnel. Basically, this printed model of an airfoil is the most important thing in this study and without it, we cannot proceed this study. After finish with the printing, a bit of finishing need to be done towards the surface of the airfoil. The airfoil is out of the printer with a bit rough surface, and since this study is concerning about the drag force on the surface of the airfoil, the surface is needed to be smoothen by applying liquid acetone that actually melting the surface of the airfoil and make it smooth. Excessive usage of the acetone might corrode the surface. Another way in smoothing the surface is using the sand paper. Here the lowest grade of sand paper were used to smooth

the surface. And as the result, the surface is smoother than when it firstly out from the printer. The surface roughness is playing important role since we are dealing with drag force so smoothing the surface is required to neglect the friction force and assuming the surface is very smooth.

3.6 Material and apparatus set up

Just like in the previous studies, this whole process of experiment will take place in a subsonic wind tunnel brand ESSOM with the model of MP130D. This subsonic wind tunnel is located inside the turbo machinery laboratory at Kompleks Makmal Kejuruteraan Mekananikal Fasa B. With the supervised of the assistant engineer in charge for the turbo machinery lab, Encik Faizal, a few weeks of experiments will be done there. The set up for this experiment is quiet simple and not to complex. It is just that the measurement specifically the angle of the slat, angle of flap, and the angle of attack of the airfoil must be accurate to obtain more precise result. In the wind tunnel, the part that will be concerned is the middle part of the wind tunnel where we place the airfoil (Figure 3.6.1). At the middle part of the wind tunnel, there is 4mm rod with thread used to mount the airfoil. This part is important in determining the result as the airfoil need to be mounted and hold strongly to avoid the airfoil shaking due to the high velocity of the air. The velocity used in this study is 9.5m/s. The velocity of the air cannot be determined directly from the speed control module (Figure 3.6.2) as it only shows the contraction section differential pressure. Contraction section differential pressure against the velocity are being used with the graph of the velocity against the net slope scale of millimeter of water (Figure 3.6.3).

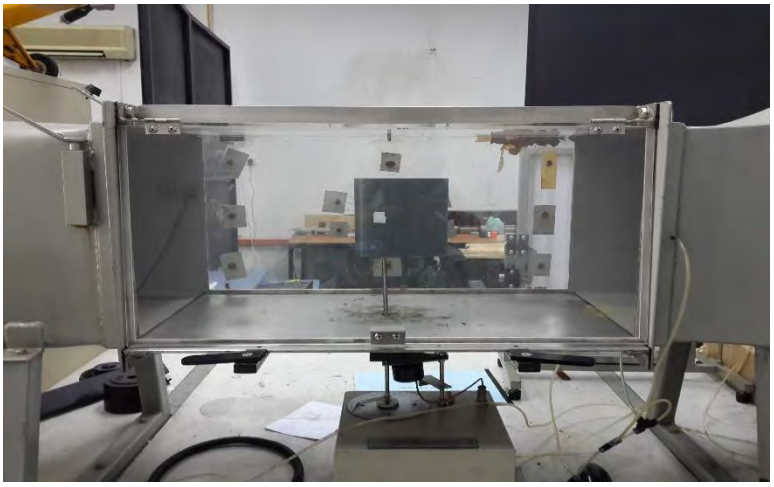

Figure 3.6.1 The middle part of the wind tunnel where subject will be tested

Figure 3.6.2 The speed control module used to control the velocity of the wind

Figure 3.6.3 Slope lever of pressure of water to determine the velocity of the air in wind tunnel

3.7 Conducting the experiment

In conducting this experiment, firstly the airfoil model will be placed inside the wind tunnel. The airfoil will be attached to the rod inside the wind tunnel (Figure 3.7.1). The rod is like a screw and the airfoil is like a thread. The airfoil was drilled and thread was made to mount the airfoil inside the wind tunnel. After perfectly mount the airfoil inside the wind tunnel, we have to set the angle of attack. This angle of attack we have to concern about the direction of flow of air and the surface of the airfoil. The angle of attack is determined by referring to the protractor on the upper wall of this transparent middle part of wind tunnel (Figure 3.7.2) First test here will take place with using the basic NACA 0015 airfoil without slat and flap. We have to test the naked airfoil to obtain data and later will be compared with the data of airfoil with slat and flap.

Figure 3.7.1 The rod inside the wind tunnel to mount the airfoil

Done with setting the airfoil inside the wind tunnel, proceed with the experiment. Plug in the plug for the power supply and then after few seconds when the system is stable, the wind tunnel can be run. In this wind tunnel system, the only thing that can be controlled directly by the user is the speed control module. This speed module control allow user to control three parameters which is the frequency, voltage and the current. We change the frequency to alter the velocity of the air. When we increase the number shown in the panel, and the parameter is selected at the frequency, the height of water at the slope will increase. The height of water increase will be measured in mm and then we have to refer to the chart provided to determine the velocity of the

air. We set the frequency to 15.00 (Figure 3.7.3). When referring to the chart, we have the velocity of air of 9.5m/s.

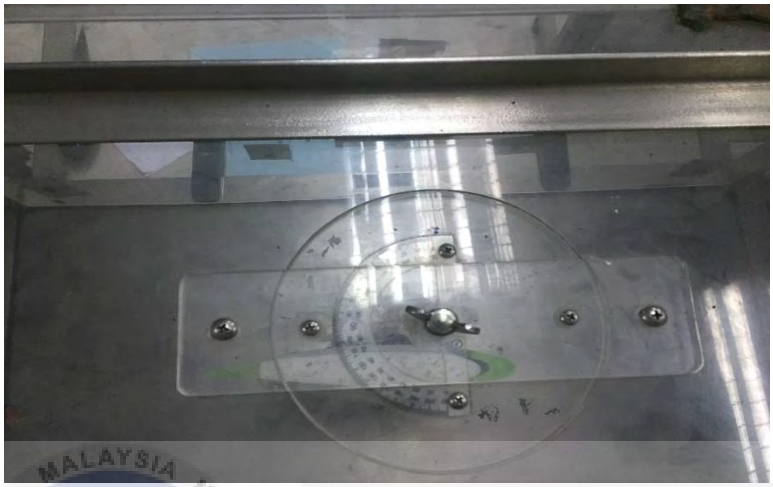

Figure 3.7.2 Protractor measure to alter the angle of attack

Figure 3.7.3 Speed control module is being set at the frequency of 15Hz

3.8 Collecting the data

For this experiment, the only data that can be obtained is the lift and drag force from the indicator module. It is quiet easy because we only have to observe some values on the module. To tabulate the data obtained, templates for the data will be printed out and brought to the laboratory. For the base case which is naked NACA 0015 airfoil, a simpler table because it only dealing with angle of attack and the forces only and one table is enough to tabulate the data (Table 3.8.1). for the experiment involving the airfoil with the leading edge slat and trailing edge flap, more table is required. A lot of experiment will be conducted as this airfoil has more changeable parameters and this will make 9 combinations of airfoil with different angle of flap and angle of slat (Table 3.8.2) and this means 9 tables 3.8.2 will be used to collect data in this study.

Table 3.8.1 the table that will be used to tabulate the data for the experiment of the base case

Angle of attack (°)	Lift Force (N)			Drag Force (N)		
	Initial	Final	Actual	Initial	Final	Actual
0						
5						
10						
15						
20						

Table 3.8.2 The table that will be used to tabulate the data for the experiment of slat and flap of an airfoil

Angle of slat (°)	Angle of flap (°)	Angle of attack (°)	Lift force (N)			Drag force (N)		
			Initial	Final	Actual	Initial	Final	Actual
		0						
		5						
		10						
		15						
		20						

CHAPTER 4

RESULT AND DISCUSSION

4.1 Introduction

The data and results obtain during the experiment will be represented in a quantitative value and it is all are tabulated. The results will be in two parts:

1. The results for the base case (NACA 0015 airfoil without slat and flap)
2. The results for the NACA 0015 airfoil with slat and flap.

4.2 Result for the base case

The base case is the origin of the problem which is involving the airfoil without any slat and flap. The experiment was conducted few times and the data are as below (Table 4.2.1)

Table 4.2.1 The data collected from the experiment of the base case

Angle of attack (°)	Lift Force (N)			Drag Force (N)		
	Initial	Final	Difference	Initial	Final	Difference
0	-0.10	-0.10	0	-0.29	-0.29	0.00
5	-0.10	-0.20	-0.1	-0.29	-0.31	-0.02
10	-0.10	-0.30	-0.2	-0.30	-0.41	-0.11
15	-0.10	-0.50	-0.4	-0.30	-0.33	-0.03
20	-0.10	-0.70	-0.6	-0.29	-0.33	-0.04

4.3 Results for the NACA 0015 airfoil with the leading edge slat and trailing edge flap

In this part, the results for the experiment involving the modified NACA 0015 which when it is attached with leading edge slat and the trailing edge flap. The details of the data from the experiment can be seen as the tables below:

1. Result for the test of 0° angle of slat and 0° angle of flap

Table 4.3.1 The data for the test with 0° angle of slat and 0° angle of flap

Angle of slat (°)	Angle of flap (°)	Angle of attack (°)	Lift force (N)			Drag force (N)		
			Initial	Final	Actual	Initial	Final	Actual
0	45	0	-0.20	-0.40	-0.2	-0.45	-0.31	0.14
		5	-0.20	-0.30	-0.1	-0.42	-0.35	0.07
		10	-0.20	0.30	0.5	-0.44	-0.22	0.22
		15	-0.40	0.20	0.6	-0.44	-0.20	0.24
		20	-0.40	0.30	-0.4	-0.40	-0.20	0.20

2. Result for the test of 0° angle of slat and 30° angle of flap

Table 4.3.2 The data for the test with 0° angle of slat and 30° angle of flap

Angle of slat (°)	Angle of flap (°)	Angle of attack (°)	Lift force (N)			Drag force (N)		
			Initial	Final	Actual	Initial	Final	Actual
0	30	0	-0.30	-0.40	-0.10	-0.38	-0.29	0.09
		5	-0.20	0.20	0.40	-0.48	-0.45	0.03
		10	-0.20	0.00	0.20	-0.39	-0.37	0.02
		15	-0.20	0.20	0.40	-0.40	-0.38	0.02
		20	0.00	0.60	0.60	-0.34	-0.20	0.14

3. Result for the test of 0° angle of slat and 45° angle of flap

Table 4.3.3 The data for the test of 0° angle of slat and 45° angle of flap

Angle of slat (°)	Angle of flap (°)	Angle of attack (°)	Lift force (N)			Drag force (N)		
			Initial	Final	Actual	Initial	Final	Actual
0	45	0	-0.20	-0.40	-0.2	-0.45	-0.31	0.14
		5	-0.20	-0.30	-0.1	-0.42	-0.35	0.07
		10	-0.20	0.30	0.5	-0.44	-0.22	0.22
		15	-0.40	0.20	0.6	-0.44	-0.20	0.24
		20	-0.40	0.30	-0.4	-0.40	-0.20	0.20

4. Result for the test of +30° angle of slat and 0° angle of flap

Table 4.3.4 The data for the test of +30° angle of slat and 0° angle of flap

Angle of slat (°)	Angle of flap (°)	Angle of attack (°)	Lift force (N)			Drag force (N)		
			Initial	Final	Actual	Initial	Final	Actual
+30 (upward)	0	0	-0.10	-0.30	-0.20	-0.54	-0.42	0.12
		5	-0.10	-0.60	-0.50	-0.54	-0.40	0.14
		10	-0.10	-0.90	-0.80	-0.48	-0.39	0.09
		15	-0.20	-1.10	-0.90	-0.49	-0.40	0.09
		20	-0.20	-1.30	-1.10	-0.51	-0.42	0.09

5. Result for the test of -30° angle of slat and 0° angle of flap

Table 4.3.5 The data for the test of -30° angle of slat and 0° angle of flap

Angle of slat (°)	Angle of flap (°)	Angle of attack (°)	Lift force (N)			Drag force (N)		
			Initial	Final	Actual	Initial	Final	Actual
-30 (downward)	0	0	-0.10	-0.40	-0.30	-0.53	-0.40	0.13
		5	-0.10	-0.80	-0.70	-0.49	-0.41	0.08
		10	-0.20	-1.10	-0.9	-0.51	-0.40	0.11
		15	-0.10	-1.00	-0.9	0.50	-0.39	-0.89
		20	-0.20	-1.00	-0.8	0.51	-0.40	-0.91

6. Result for the test of +30° angle of slat and 45° angle of flap

Table 4.3.6 The data for the test of +30° angle of slat and 45° angle of flap

Angle of slat (°)	Angle of flap (°)	Angle of attack (°)	Lift force (N)			Drag force (N)		
			Initial	Final	Actual	Initial	Final	Actual
+30 (upward)	45	0	-0.10	-0.50	-0.40	-0.46	-0.27	0.19
		5	0.00	-0.60	-0.60	-0.44	-0.30	0.14
		10	-0.20	0.40	0.60	-0.22	0.02	0.24
		15	-0.20	0.50	0.70	-0.19	0.04	0.23
		20	-0.20	0.50	0.70	-0.20	0.11	0.31

7. Result for the test of -30° angle of slat and 45° angle of flap

Table 4.3.7 The data for the test of -30° angle of slat and 45° angle of flap

Angle of slat (°)	Angle of flap (°)	Angle of attack (°)	Lift force (N)			Drag force (N)		
			Initial	Final	Actual	Initial	Final	Actual
-30 (downward)	45	0	-0.30	-0.20	0.10	-0.21	-0.10	0.11
		5	-0.20	0.10	0.30	-0.21	-0.11	0.10
		10	-0.20	0.20	0.40	-0.22	-0.08	0.14
		15	-0.20	0.30	0.50	-0.19	-0.02	0.17
		20	-0.20	0.50	0.70	-0.17	0.02	0.19

8. Result for the test of 0° angle of slat and 30° angle of flap

Table 4.3.8 The data for the test of -30° angle of slat and 30° angle of flap

Angle of slat (°)	Angle of flap (°)	Angle of attack (°)	Lift force (N)			Drag force (N)		
			Initial	Final	Actual	Initial	Final	Actual
0	30	0	-0.10	-0.10	0.00	-0.20	-0.14	0.06
		5	-0.20	0.00	0.20	-0.22	0.13	0.35
		10	-0.10	0.10	0.20	-0.19	-0.11	0.08
		15	-0.20	0.20	0.40	-0.19	-0.09	0.10
		20	-0.20	0.40	0.60	-0.19	-0.05	0.14

9. Result for the test of 30° angle of slat and 30° angle of flap

Table 4.3.9 The data for the test of +30° angle of slat and 30° angle of flap

Angle of slat (°)	Angle of flap (°)	Angle of attack (°)	Lift force (N)			Drag force (N)		
			Initial	Final	Actual	Initial	Final	Actual
+30 (upward)	30	0	-0.20	-0.20	0.00	-0.21	-0.14	0.07
		5	-0.20	0.00	0.20	-0.19	-0.12	0.07
		10	-0.10	0.20	0.30	-0.17	-0.09	0.08
		15	-0.20	0.30	0.50	-0.17	-0.06	0.11
		20	-0.20	0.40	0.60	-0.17	-0.03	0.14

The data obtained above are from the test of the airfoil with the leading edge slat and the trailing edge flap. The combination of various angle of slat and flap produce 9 different configuration of the airfoil that gives different result from the experiment. The further detailed discussion of the data will be discussed.

4.4 Analysis of the base case

From the data obtained from the Table 4.2.1, we can see that the values of the difference between final and initial value of the lift force which represent the actual lift force acting on the airfoil are decreasing as it goes down the zero with negative value. The sign negative actually does not represent the value as it only indicates the direction of the airfoil. Since the negative sign only representing the direction of the force, so the sign can be neglected in analysis. From the chart below, we can see that the value of the lift force is increasing directly proportional to the angle of attack. For the drag force, the value is increasing as the angle of attack increase from 0° to 10° and as the angle of attack increase from 10°, the value of drag force decrease. The range value of drag force is small and ranging below 0.1.

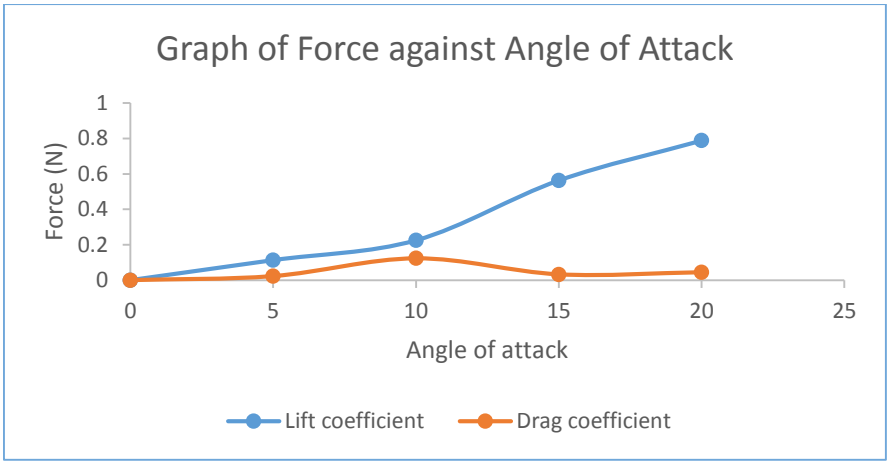

Chart 4.4.1 Graph of angle of attack against the lift and drag force.

From the value of drag force and lift force obtained, the value of lift and drag coefficient can be calculated further using the mathematical equation for the drag and lift force. Value of drag coefficient, C_D can be calculated using the equation of :

$$C_D = \frac{F_D}{\frac{1}{2} v^2 A \rho} \qquad C_L = \frac{F_L}{\frac{1}{2} v^2 A \rho}$$

Where F_D is the drag force, F_L is the lift force v is the velocity of the air inside wind tunnel, A is the contact area of the airfoil with the air and ρ is the density of the air. From the experiment of this base case, the velocity of air is 9.5 m/s and the density of air is 1.1644 kg/m^3. The table of the lift and drag coefficient and angle of attack can be seen as in Table 4.4.1 and the analysis of the data is at the Chart 4.4.1.

Table 4.4.1 The table of angle of attack and the drag and lift coefficient

Angle of attack	Lift		Drag	
	Lift Force (N)	Lift coefficient	Drag force (N)	Drag coefficient
0	0.00	0.000	0.00	0.000
5	-0.10	0.113	-0.02	0.023
10	-0.20	0.225	-0.11	0.124
15	-0.50	0.563	-0.03	0.033
20	-0.70	0.788	-0.04	0.045

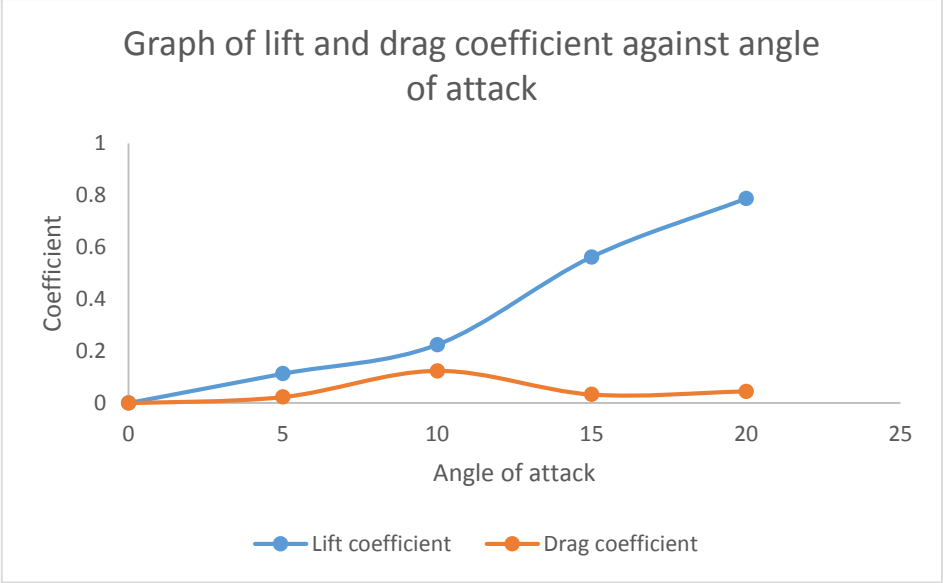

Chart 4.4.1 Graph of coefficient against angle of attack

From the chart above, we can sell that the value of lift coefficient is increasing directly proportional to the angle of attack. For the value of drag coefficient, it is increasing slightly as the angle of attack being increase until 10° and as the angle keep increasing, the value keep dropping with a small value.

4.5 Analaysis of leading edge slat and trailing edge flap

The data obtained in the Table 4.3.1 until Table 4.3.9 are all from the experiment of 9 different configuration of the leading edge slat and the trailing edge flap. From the data we can say that each configuration of slat and flap will produce different lift and drag force towards the aerodynamic performance of the airfoil. Every parameters that can be change will cause different effect on the airfoil especially to the lift and drag force acting on the airfoil. The further analysis can be seen as in the charts below.

Case 1 : 0° angle of slat, 0° angle of flap

The first case of this slat and flap application on airfoil is when the airfoil is attached with a leading edge slat and trailing edge flap where both slat and flap are at the angle of attack of 0°.

The data of the lift and drag coefficient for this configuration can be seen as in Table 4.5.1.

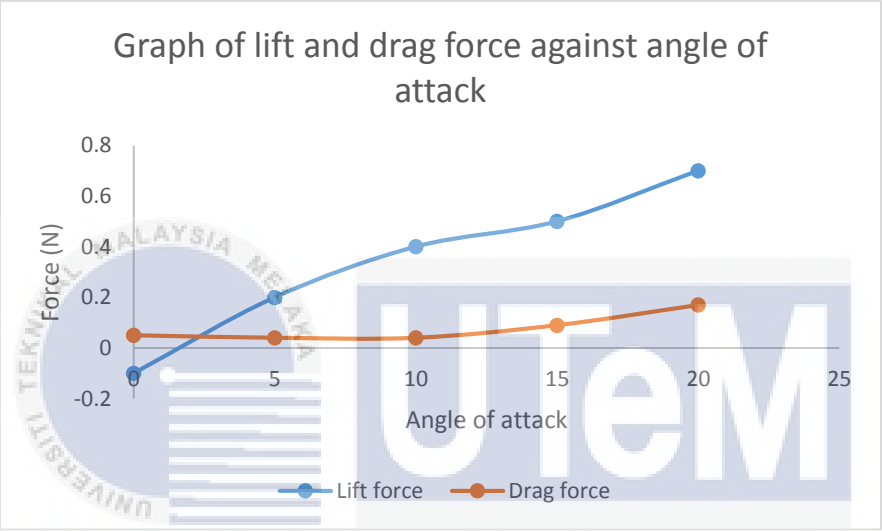

Chart 4.5.1 Graph of force against angle of attack for test 1

The lift force acting on the airfoil is at its max when the angle of attack of the airfoil configuration is at 20°. For the value of drag force, it can be seen that the drag force change is small for the change of angle of attack from 0° to 10° and as angle of attack increase to 15°, the value of drag force increases significantly and the drag reaches its max at the angle of attack of 20°.

The further analysis can be done by doing the calculation to find the lift and drag coefficient. The lift and drag formula can be used to determine the value of lift and drag coefficient. This configuration of airfoil gives the area of the airfoil surface larger with the area of 0.0208 m^2. The other parameters are still the same with the base case with velocity of air of 9.5 m/s, density of air at room temperature of 1.1644 kg/m^3

$$C_D = \frac{F_D}{\frac{1}{2} v^2 A \rho} \qquad C_L = \frac{F_L}{\frac{1}{2} v^2 A \rho}$$

The data of the lift and drag coefficient for this configuration can be seen as in Table 4.5.1.

Table 4.5.1 Lift and drag coefficient for test 1

Angle of attack (°)	Lift		Drag	
	Lift Force (N)	Lift coefficient	Drag force (N)	Drag coefficient
0	-0.10	0.090	0.05	0.046
5	0.20	0.183	0.04	0.036
10	0.40	0.366	0.04	0.036
15	0.50	0.457	0.09	0.082
20	0.70	0.640	0.17	0.155

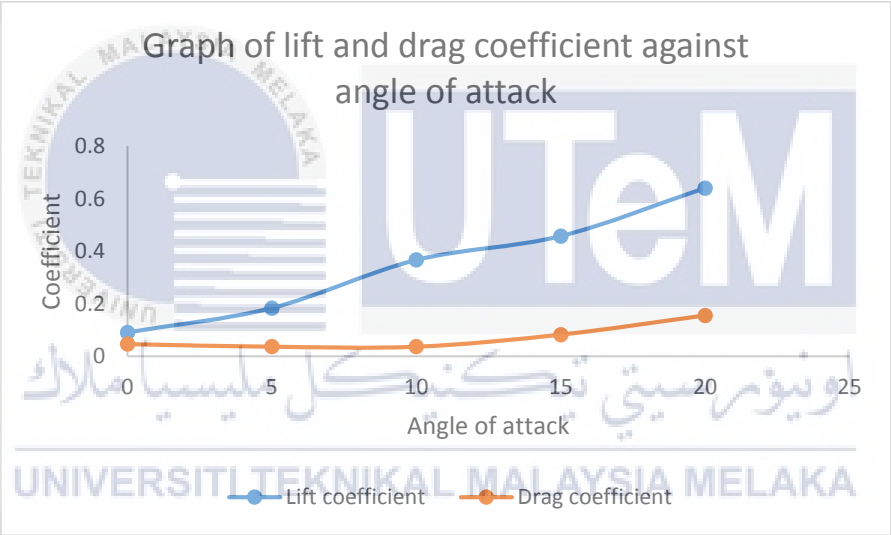

Chart 4.5.2 Graph of lift and drag coefficient against angle of attack

From the chart above, both value of the lift and drag coefficient are increasing as the angle of attack increases. However, the increasing value is difference. The value of lift coefficient is large as double the value of the drag coefficient. The range of value of the drag coefficient is small which is from 0.046 to 0.155 compared to the range of lift coefficient which is range from 0.09 to 0.640. This means that the angle of attack affects the value of lift coefficient more compared to its effect towards the drag force.

Case 2: 0° angle of slat, 30° angle of flap

This second case is when the airfoil is attached to the slat with 0° angle and the trailing edge with the angle of 30°. This configuration is like the first case but this one with the trailing edge flap being bend downward with the angle of 30°. The data for the lift and drag force and its drag and lift coefficient obtained during this test are as in Table 4.5.2

Table 4.5.2 The lift and drag coefficient for test 2

Angle of attack (°)	Lift		Drag	
	Lift Force (N)	Lift coefficient	Drag force (N)	Drag coefficient
0	-0.10	0.091	0.09	0.082
5	0.40	0.366	0.03	0.027
10	0.20	0.183	0.02	0.018
15	0.40	0.366	0.02	0.018
20	0.60	0.549	0.14	0.128

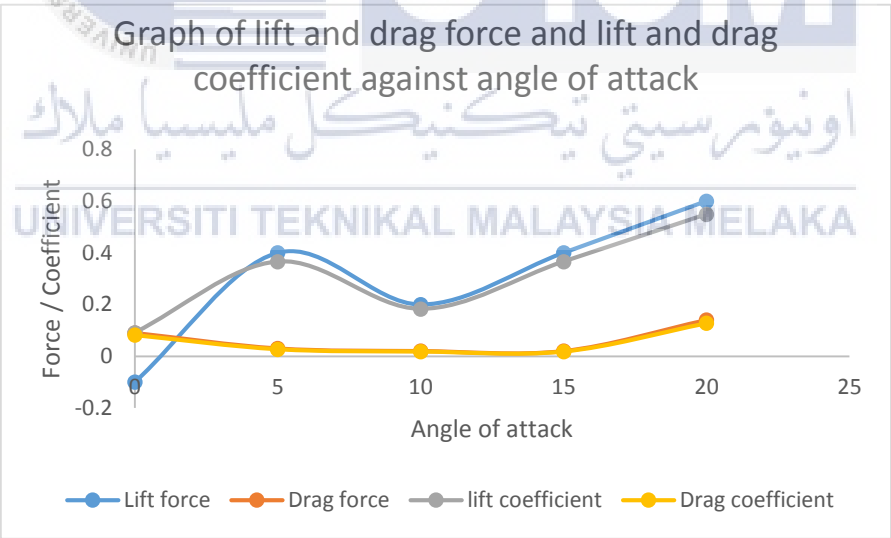

Chart 4.5.3 Graph of lift and drag force & lift and drag coefficient

From the chart above, we can see that both drag force and drag coefficient value changes are almost same with a very small of difference and for the lift, both lift coefficient and lift force also in the same shape. The value of lift coefficient and drag coefficient both are at their maximum when the angle of attack if the airfoil is at 20°.

Case 3: 0 angle of slat, 45 angle of flap

In this test, the condition is almost same like the previous case just the different is the angle of flap is larger. The flap is bent to the angle of 45°. The data for the lift and drag coefficient are as in Table 4.5.3 below

Table 4.5.3 The lift and drag coefficient for the test 3

Angle of attack (°)	Lift		Drag	
	Lift Force (N)	Lift coefficient	Drag force (N)	Drag coefficient
0	-0.20	0.183	0.14	0.128
5	-0.10	0.091	0.07	0.064
10	0.50	0.457	0.22	0.201
15	0.60	0.549	0.24	0.219
20	-0.40	0.366	0.20	0.183

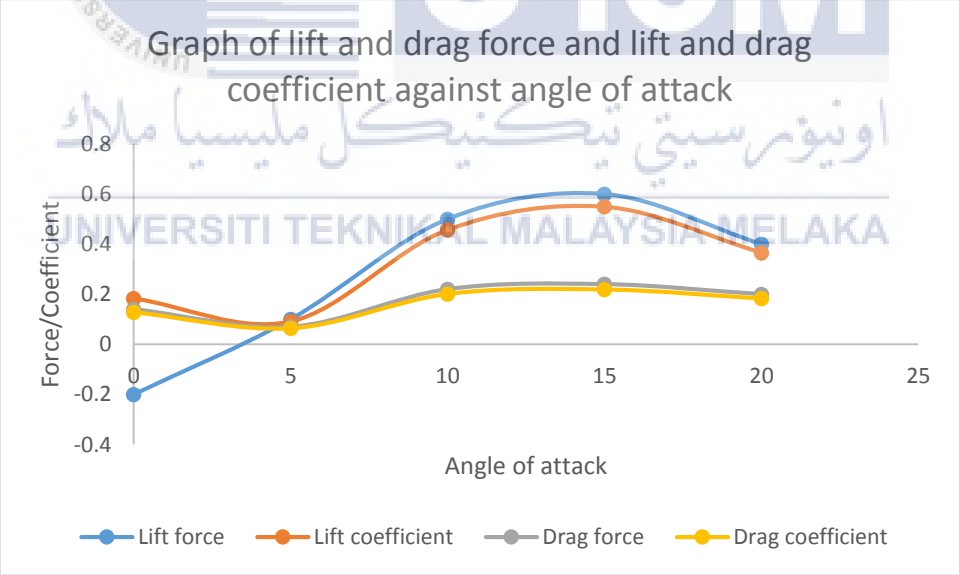

Chart 4.5.4 Graph of lift and drag force & lift and drag coefficient

From the chart plotted, we can see that the two components of lift which is the lift force and lift coefficient value are almost the same after the angle of attack of 5°. And for the drag force and coefficient, the value are almost the same from the beginning until the end. Only small difference for the value of the drag components.

Case 4: +30° angle of slat, 0° angle of flap

The positive angle indicates the direction of the deflection. Since the airfoil is mounted inside the wind tunnel vertically, the positive angle of 30° indicates that the angle of salt is being deflected by 30° to the left. The angle of flap however is left at 0 angle which means remain unchanged. The data for the lift and drag force from the experiments and the data for lift and drag coefficient from the calculation are is the Table 4.5.4

Table 4.5.4 The lift and drag coefficient for the test 4

Angle of attack (°)	Lift		Drag	
	Lift Force (N)	Lift coefficient	Drag force (N)	Drag coefficient
0	-0.20	0.183	0.11	0.100
5	-0.50	0.467	0.14	0.128
10	-0.80	0.732	0.09	0.082
15	-0.90	0.823	0.09	0.082
20	-1.10	1.006	0.09	0.082

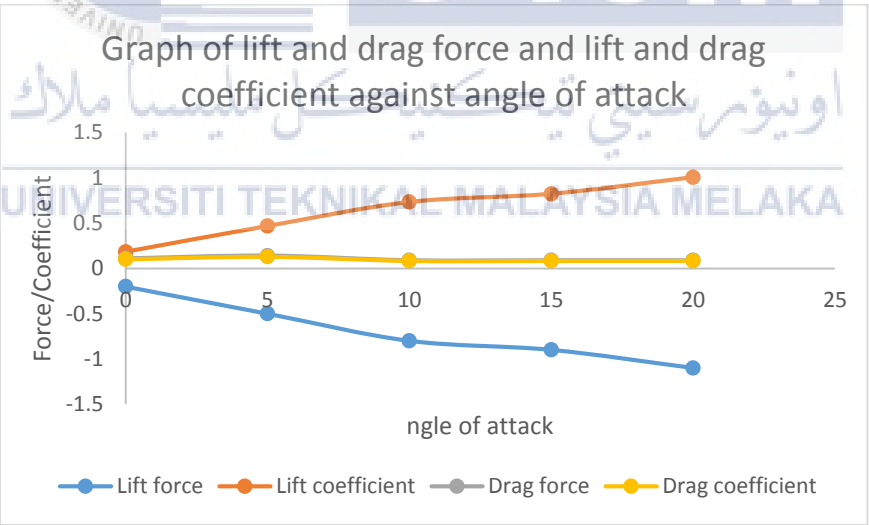

Chart 4.5.3 Graph of lift and drag force & lift and drag coefficient

In this case, we can see the lift components are having 2 opposite value where at the same angle of attack, lift force and lift coefficient are having same value but the difference is thsign while the drag components are having almost same value throughout all the angle of attack.

Case 5: -30° angle of slat, 0° angle of flap

This study is the inverse of the previous case. Previous case we have a positive angle of slat which means the slat is deflect upwards while this case is where the slat is being deflected downwards with the deflection of angle of 30°. Table 4.5.5 shows the data from the experiment and from the calculation.

Table 4.5.5 The lift and drag coefficient for the test 5

Angle of attack (°)	Lift		Drag	
	Lift Force (N)	Lift coefficient	Drag force (N)	Drag coefficient
0	-0.30	0.274	0.13	0.119
5	-0.70	0.640	0.08	0.073
10	-0.90	0.823	0.11	0.101
15	-0.90	0.823	-0.89	0.814
20	-0.80	0.731	0.91	0.833

From the data obtained, graph was plotted to analyze the lift and drag coefficient. From Chart 4.5.4 below, lift force and coefficient having inverse value to each other with a small difference and the drag component keeps almost same value from the angle of attack of 0 to 10 and started to drifting apart at the angle of 15° converge back having small difference in value at the angle of attack of 20°.

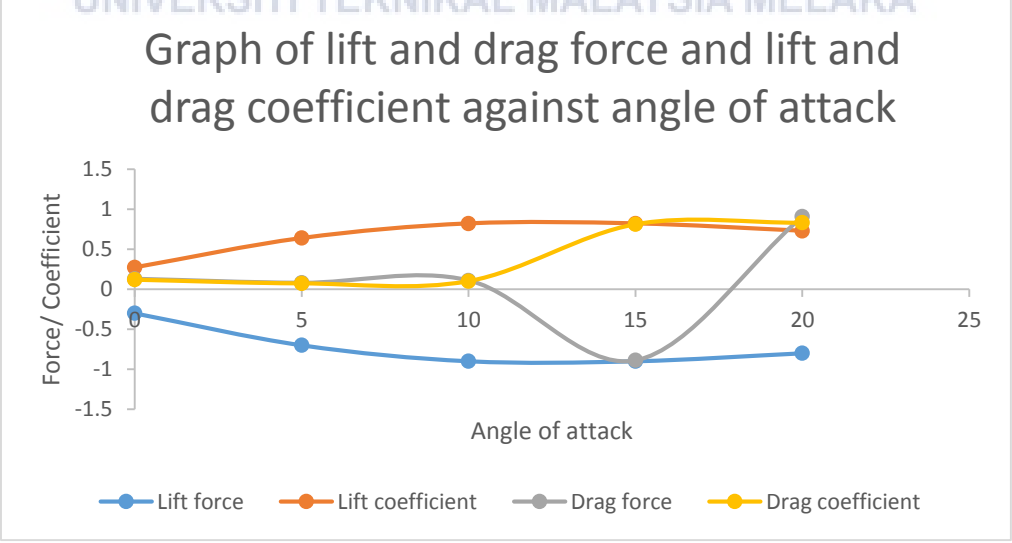

Chart 4.5.4 Graph of lift and drag force & lift and drag coefficient

Case 6: +30° angle of slat, 45° angle of flap

In this case, both angle of slat and angle of flap are deflected to large angle of deflection. 30° for the salt and 45° for the flap. The data from the experiments and the data of lift and drag coefficient from further calculation are as in Table 4.5.6

Table 4.5.6 The lift and drag coefficient for the test 6

Angle of attack (°)	Lift		Drag	
	Lift Force (N)	Lift coefficient	Drag force (N)	Drag coefficient
0	-0.40	0.366	0.19	0.173
5	-0.60	0.549	0.14	0.128
10	0.6	0.549	0.24	0.219
15	0.7	0.640	0.23	0.210
20	0.7	0.640	0.31	0.283

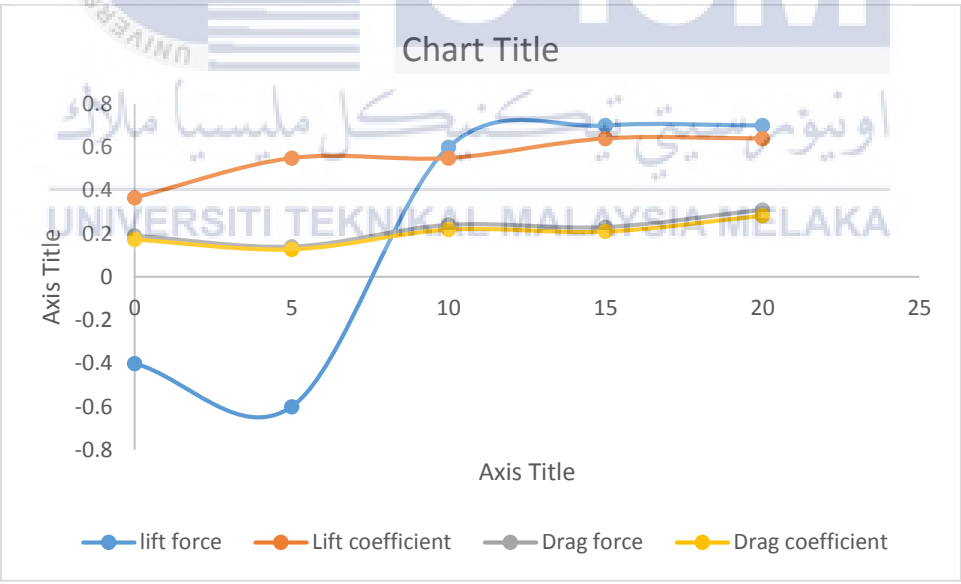

Chart 4.5.5 Graph of lift and drag force & lift and drag coefficient

For this case of experiment, the drag components are seems likely to have almost same value of force and coefficient and for the lift components, it starts with inversely signed from the angle of attack of 0° to 5° but entering the angle of 10°, the lift force and lift coefficient had almost same value until the angle of 20°.

Case 7: -30° angle of slat, 30° angle of flap

In this case of experiment, the slat and the flap will have the same angle of deflection. The slat is being deflected on -30° which means it is deflected downward facing the air flow while the flap will deflect 30° it its direction. The data obtained later being recorded and further calculation are also being done to estimate the value of drag and lift coefficient.

Table 4.5.7 The lift and drag coefficient for the test 7

Angle of attack (°)	Lift		Drag	
	Lift Force (N)	Lift coefficient	Drag force (N)	Drag coefficient
0	0.10	0.091	0.11	0.100
5	0.30	0.275	0.10	0.091
10	0.40	0.366	0.14	0.128
15	0.50	0.457	0.17	0.155
20	0.70	0.640	0.19	0.173

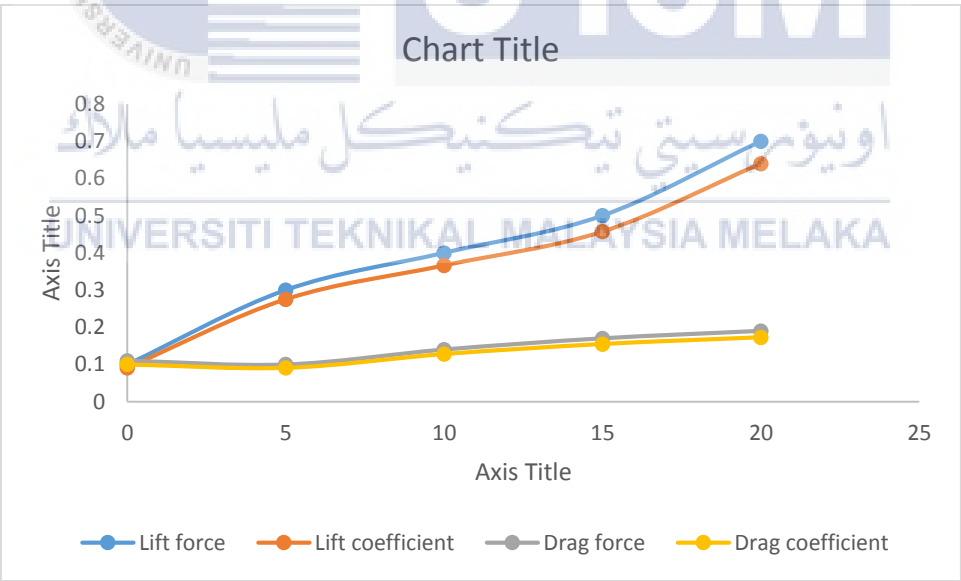

Chart 4.5.6 Graph of lift and drag force & lift and drag coefficient

The lift components and drag components both are having almost similar value since the graphs are very close to each other. Only small value that differs the value of drag lift and drag coefficient

Case 8: 30 angle of slat, 30 angle of flap

In this case of experiment, the slat is being set at its normal which is at 0° angle facing the air flow and the flap is being deflected at the angle of 30°. The data from the experiments and the data of lift and drag coefficient from further calculation are as in Table 4.5.8

Table 4.5.8 The lift and drag coefficient for the test 8

Angle of attack (°)	Lift		Drag	
	Lift Force (N)	Lift coefficient	Drag force (N)	Drag coefficient
0	0.00	0.00	0.06	0.055
5	0.20	0.183	0.35	0.320
10	0.20	0.183	0.08	0.073
15	0.40	0.366	0.10	0.091
20	0.60	0.549	0.14	0.128

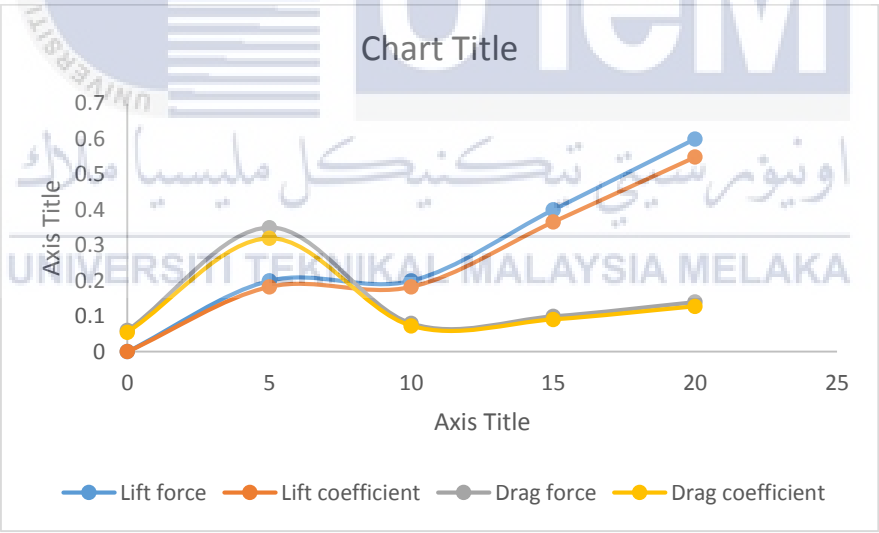

Chart 4.5.7 Graph of lift and drag force & lift and drag coefficient

From the chart, we can see that the pattern of the force and coefficient of lift are almost the same. The graph has the same shape for the drag components. The same thing happens to the lift components too where the graph shape are almost the same that is different with a small value. The lift force is the highest at the angle of 20° and the value of drag force is decrease as the angle of attack is increased from 5° to 10°.

Case 9: +30 angle of slat, 30 angle of flap

In this experiment, the set up was the slat is being lifted by 30° upwards facing the air flow and the angle of flap was being deflected for the angle of 30°.

Table 4.5.9 The lift and drag coefficient for the test 9

Angle of attack (°)	Lift		Drag	
	Lift Force (N)	Lift coefficient	Drag force (N)	Drag coefficient
0	0.00	0.000	0.07	0.064
5	0.20	0.183	0.07	0.064
10	0.30	0.274	0.08	0.731
15	0.50	0.457	0.11	0.100
20	0.60	0.549	0.14	0.128

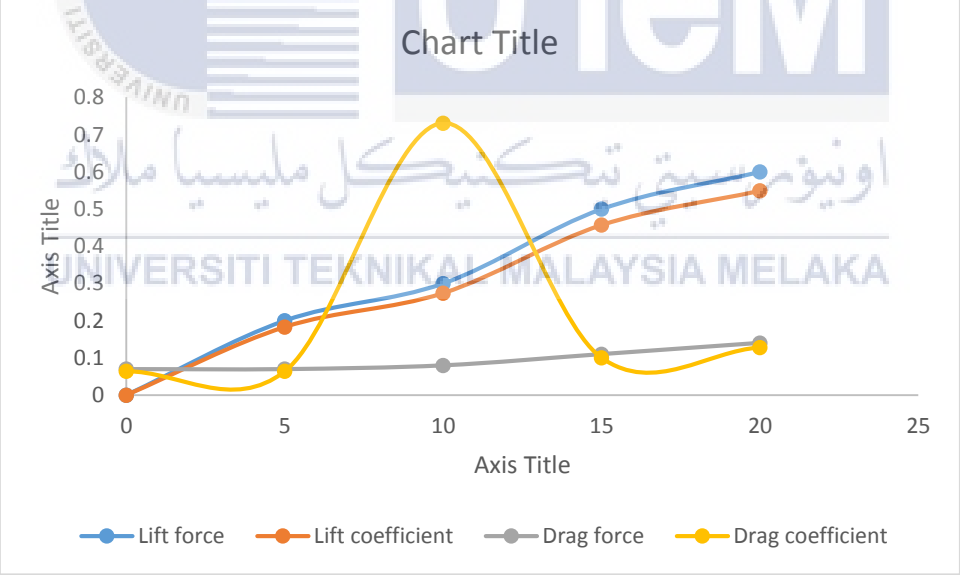

Chart 4.5.8 Graph of lift and drag force & lift and drag coefficient

At the angle of attack of 10°, the value of drag force and drag coefficient are drifted apart, the drag was really small and the drag coefficient value at that angle of attack was really high. As the angle of attack being increased from 10° to 15°, the value of drag components approaching each other with a very small value of difference. On the other hand, the lift components maintaining close value to each other from the beginning until the angle of attack of 20°.

CHAPTER 5

CONCLUSION

5.1 Overview

In this chapter, a conclusion will be made based on the experiments that had been conducted during the last few weeks at the turbo machinery laboratory at Kompleks Makmal Kejuruteraan Mekanikal Fasa B, UTeM. At the same time, the objectives of this study are also will be looked back and will find out whether this study achieved its objectives or not.

5.2 Base case

Base case is the experiment involving the testing of the NACA 0015 without its leading edge slat and trailing edge flap airfoil inside a subsonic wind tunnel. Since there is nothing that can be change on the airfoil, basically this base case experiment is about studying the effect of different angle of attack towards the airfoil. In this study, a range of angle of attack from 0° to 20° with the interval of 5° was conducted. The data obtained from the test was the lift and the drag force and from it, the further calculation was done to measure the coefficient of lift and drag on the airfoil. The data is then being analyze as in Chart 5.2.1 so that it can be interpret easily.

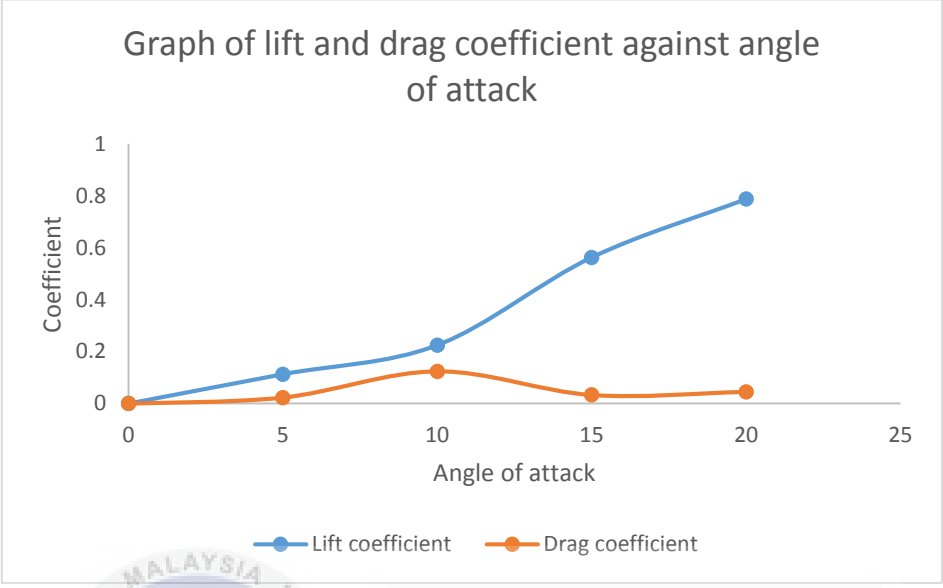

Chart 5.2.1 The graph of coefficient of drag and lift for base case.

From the chart we can see the coefficient of lift and drag of the airfoil at different angle of attack. From the test, the airfoil produce its maximum lift coefficient at the angle of attack of 20°. At his angle of attack, the lift coefficient is the highest, hence the highest lift force was produced at this angle o attack. Following the equation for the lift coefficient, the lift force is directly proportional to the lift coefficient and this base case is following that statement. The highest lift coefficient produced with the highest lift force.

For the drag components, we can see from the chart that the values of drag coefficient throughout five different angle of attack are almost constant it is just at a point of angle of attack of 10, the drag coefficient is high. The drag force is considered as low in this study because of the airfoil does not have flap. Flaps are a type of high-lift device used to increase the lift of an aircraft wing at a given airspeed. Without the flap, the lift force produce is not as much as with it.

While cruising at high altitude, normally plane will retract its wing flap in order to reduce the drag force acing on it. Flap is really helping during the take off because it can help increase the lift on the wing but during cruise, flap is a no since it increase the drag force acting on the

plane which indirectly will reduce plane's speed and increasing the fuel consumption because more power needed to achieve the desired velocity.

5.3 Effect of leading edge slat and trailing edge flap

From the series of experiments that was involving several arrangements for the configuration of the airfoil inside the wind tunnel, we can find out that when the airfoil is equipped with the leading edge slat and the trailing edge flap it will have different experimental result compared to the base case. Some arrangement can give a better aeronautic performance on the airfoil while some arrangements are only making the airfoil being less efficient than the base case.

We look at the case 1 first, the arrangement of the airfoil with 0° angle of slat and 0° angle of flap. At first the value of lift coefficient produced was small until the angle of attack o f the airfoil is being lifted from 0° to 20°. At the angle of 20°, the value of lift coefficient was high hence it produced a high lift force. High lift on airfoil is a something that is good because high lift means easier for it to take off. At the same time, the value for the drag components produced on this configuration are not really a good value because the value of drag produced is large. Large drag means it is harder to take off because of the opposite drag force acting on the airfoil.

From the experiments that have been conducted, I found out that the best configuration from the 9 different configurations is the configuration for case 4 where the leading edge slat has the angle of 30 and the flap is remain at 0. For this configuration, the lift produced was the highest of all case. The highest lift coefficient produced was 1.006 with the lift force of 1.10 N. the detailed data for this case are as in table 5.3.1 below.

Table 5.3.1 The data for the case 4 experiment

Angle of attack (°)	Lift		Drag	
	Lift Force (N)	Lift coefficient	Drag force (N)	Drag coefficient
0	-0.20	0.183	0.11	0.100
5	-0.50	0.467	0.14	0.128
10	-0.80	0.732	0.09	0.082
15	-0.90	0.823	0.09	0.082
20	-1.10	1.006	0.09	0.082

On the other hand, while producing high lift coefficient, this arrangement were also producing small value of drag. Even the value of drag component produced is not the best which is the smallest just like in case 2 where the drag coefficient produced was 0.018 at the angle of attack of 10°. The arrangement for case 4 is where the angle of slat is being lifted upwards facing the flow and the angle of flap is being remain at 0° angle.

5.4 Conclusion and recommendation

As a conclusion, from the review of the previous study and from my own experiments, one thing for sure that I can say is the leading edge slat and the trailing edge flap do effect the aerodynamic performance of an NACA 0015 airfoil. The term effect here means it is either can improve the performance of the airfoil or it might also reduce the performance of the airfoil depending on the many conditions that can be considered such as the velocity of air and the angle of attack.

For the recommendation, I would like to suggest that future research on this related topic should be done more and more to improve the performance of airfoil in wide fields. The research that will be done in the future should cover a wider scope and with the future technologies that will be much modern, I am pretty sure there will be a lot of things that can be explored in order to improve the performance of the airfoil.

REFERENCES

Li, C., Dong, H., & Liu, G. (2015). Effects of a dynamic trailing-edge flap on the aerodynamic performance and flow structures in hovering flight. *Journal of Fluids and Structures*, *58*, 49–65. https://doi.org/10.1016/j.jfluidstructs.2015.08.001

Nati, G., Kotsonis, M., Ghaemi, S., & Scarano, F. (2013). Control of vortex shedding from a blunt trailing edge using plasma actuators. *Experimental Thermal and Fluid Science*, *46*, 199–210. https://doi.org/10.1016/j.expthermflusci.2012.12.012

Pagani, C. C., Souza, D. S., & Medeiros, M. A. F. (2017). Experimental investigation on the effect of slat geometrical configurations on aerodynamic noise. *Journal of Sound and Vibration*, *394*, 256–279. https://doi.org/10.1016/j.jsv.2017.01.013

Şahin, İ., & Acir, A. (2015). Numerical and Experimental Investigations of Lift and Drag Performances of NACA 0015 Wind Turbine Airfoil. *International Journal of Materials, Mechanics and Manufacturing*, *3*(1), 22–25. https://doi.org/10.7763/IJMMM.2015.V3.159

Savory, E., Toy, N., Tahouri, B., & Dalley, S. (1992). Flow regimes in the cove regions between a slat and wing and between a wing and flap of a multielement airfoil. *Experimental Thermal and Fluid Science*, *5*(3), 307–316. https://doi.org/10.1016/0894-1777(92)90075-G

Weishuang, L., Yun, T., & Peiqing, L. (2017). Aerodynamic optimization and mechanism design of flexible variable camber trailing-edge flap, (April).